Recent Advances in the Numerical Solution of Hamiltonian Partial Differential Equations

Recent Advances in the Numerical Solution of Hamiltonian Partial Differential Equations

Luigi Barletti[1,b)], Luigi Brugnano[1,a)], Gianluca Frasca Caccia[2,c)] and Felice Iavernaro[3,d)]

[1]*Dipartimento di Matematica e Informatica "U. Dini", Università di Firenze, Firenze, Italy.*
[2]*School of Mathematics, Statistics & Actuarial Science, University of Kent, Canterbury, UK.*
[3]*Dipartimento di Matematica, Università di Bari, Bari, Italy.*

[a)]Corresponding author: luigi.brugnano@unifi.it
[b)]luigi.barletti@unifi.it
[c)]g.frasca-caccia@kent.ac.uk
[d)]felice.iavernaro@uniba.it

Abstract. In this paper, we study recent results in the numerical solution of Hamiltonian partial differential equations (PDEs), by means of energy-conserving methods in the class of *Line Integral Methods*, in particular, the Runge-Kutta methods named *Hamiltonian Boundary Value Methods (HBVMs)*. We show that the use of energy-conserving methods, able to conserve a discrete counterpart of the Hamiltonian functional (which derives from a proper space semi-discretization), confers more robustness to the numerical solution of such problems.

INTRODUCTION

The numerical solution of Hamiltonian problems has been the subject of many researches in the last decades, within the framework of the so called *Geometric Integration*. At the beginning, the focus was mainly on ODE problems, where fundamental results, concerning symplectic and (more recently) energy-conserving methods, have been derived. Later on, the investigation has also moved towards the setting of Hamiltonian PDEs, where symplectic [21], multi-symplectic [18] and, more recently, energy-conserving methods, have been studied. In particular, we are here concerned with some recent achievements concerning the use of energy-conserving methods in the HBVMs class [4, 6], which prove to be effective and reliable.

HBVMs are energy-conserving Runge-Kutta methods derived in the framework of *discrete line integral methods*, at first introduced in [15, 16, 17], and then developed in [7, 10, 12] (see also [8, 3] for the efficient implementation of HBVMs). For a comprehensive introduction to such methods, we refer to the recent monograph [6].

In this paper, we consider the application of HBVMs for numerically solving Hamiltonian PDEs, with particular reference to the *semilinear wave equation*,

$$u_{tt}(x,t) = u_{xx}(x,t) - f'(u(x,t)), \qquad (x,t) \in \Omega \equiv [a,b] \times [0,\infty), \tag{1}$$

(with f' the derivative of f) and the *nonlinear Schrödinger equation*, which we write in the general form[1]

$$i\psi_t(x,t) + \psi_{xx}(x,t) + f'\left(|\psi(x,t)|^2\right)\psi(x,t) = 0, \qquad (x,t) \in \Omega, \tag{2}$$

(with i denoting, as usual, the imaginary unit) which constitute significant instances of such problems. In both cases, the problem is defined by considering suitable initial and periodic boundary conditions, i.e.,

$$u(x,0) = u_0(x), \quad u_t(x,0) = v_0(x) \qquad x \in [a,b], \qquad u(a,t) = u(b,t), \quad u_x(a,t) = u_x(b,t), \qquad t > 0, \tag{3}$$

[1]In the typical case, $f(s) = \kappa s^2$, with $\kappa = \pm 1$, depending on the fact that one is dealing with the *focusing* or *defocusing* case.

for (1), and

$$\psi(x,0) = \psi_0(x) \equiv u_0(x) + iv_0(x), \qquad x \in [a,b], \qquad \psi(a,t) = \psi(b,t), \quad \psi_x(a,t) = \psi_x(b,t), \qquad t > 0, \tag{4}$$

for (2). Moreover, we shall assume that the spatial interval is finite, i.e., $-\infty < a < b < +\infty$. It is worth mentioning that also the case of an infinite interval could be, in principle, tackled, by considering different computational paradigms (e.g., [22, 23, 24]). Equations (1) and (2) can be cast in Hamiltonian form, by setting

$$v(x,t) := u_t(x,t), \quad \text{for (1)}; \qquad \psi(x,y) \equiv u(x,t) + iv(x,t), \quad \text{for (2)}; \qquad y = (u,\, v)^\top,$$

as follows:

$$y_t = J\nabla\mathcal{H}[y], \qquad \text{with} \qquad J = \begin{pmatrix} 0 & 1 \\ -1 & 0 \end{pmatrix}, \qquad \text{and} \qquad \nabla\mathcal{H} = \left(\frac{\delta}{\delta u}\mathcal{H}, \quad \frac{\delta}{\delta v}\mathcal{H} \right)^\top$$

the vector of the functional derivatives of the *Hamiltonian functional* $\mathcal{H}[y] \equiv \mathcal{H}[u,v]$.[2] It can be easily checked that, because of the periodic boundary conditions,

$$\mathcal{H}[u,v] = \frac{1}{2}\int_a^b \left(v^2 + u_x^2 + 2f(u)\right) \mathrm{d}x = \frac{1}{2}\int_a^b \left(v^2 - uu_{xx} + 2f(u)\right) \mathrm{d}x, \tag{5}$$

$$\mathcal{H}[u,v] = \frac{1}{2}\int_a^b \left(v_x^2 + u_x^2 - f\left(u^2+v^2\right)\right) \mathrm{d}x = -\frac{1}{2}\int_a^b \left(vv_{xx} + uu_{xx} + f\left(u^2+v^2\right)\right) \mathrm{d}x, \tag{6}$$

for (1) and (2), respectively. We also consider the quadratic functionals

$$\mathcal{J}[u,v] = \int_a^b (u_x v)\, \mathrm{d}x, \qquad \mathcal{M}[u,v] = \int_a^b \left(u^2+v^2\right) \mathrm{d}x. \tag{7}$$

$\mathcal{J}$ represents the momentum, for (1), whereas $\mathcal{M}$ represents the mass (i.e., the probability density), for (2). It is quite easy to prove the following result.

Theorem 1 *For problem (1)-(3) one has (see (5) and (7)):*

$$\mathcal{H}[u,v](t) = \mathcal{H}[u,v](0), \qquad \mathcal{J}[u,v](t) = \mathcal{J}[u,v](0), \qquad \forall t > 0.$$

For problem (2)-(4) one has (see (6) and (7)):

$$\mathcal{H}[u,v](t) = \mathcal{H}[u,v](0), \qquad \mathcal{M}[u,v](t) = \mathcal{M}[u,v](0), \qquad \forall t > 0.$$

In other words, (5), (6), and (7) provide *conservation laws* for the corresponding problems.[3]

In the following sections we consider, at first, the numerical solution of (1)-(3), then moving to (2)-(4). Later on, we sketch the main facts about HBVMs and, finally, we report some numerical tests and final conclusions.

SPACE SEMI-DISCRETIZATION FOR THE SEMILINEAR WAVE EQUATION

In order to numerically solve (1)-(3), we shall use a Fourier-Galerkin space semi-discretization, by expanding the solution along the following periodic orthonormal basis for $L^2[a,b]$,[4]

$$c_0(x) \equiv \frac{1}{\sqrt{b-a}}, \qquad c_j(x) = \sqrt{\frac{2}{b-a}} \cos\left(2j\pi\, \frac{x-a}{b-a}\right), \quad s_j(x) = \sqrt{\frac{2}{b-a}} \sin\left(2j\pi\, \frac{x-a}{b-a}\right), \quad j = 1,2,\ldots, \tag{8}$$

[2] We shall use either one or the other notation, when convenient. Moreover, we shall sometimes omit the arguments, to simplify the notation.

[3] A further quadratic invariant, similar to the momentum, also exists for the nonlinear Schrödinger equation, though we shall not consider it here.

[4] We shall consider different space discretizations elsewhere.

thus obtaining:

$$u(x,t) = \gamma_0(t)c_0(x) + \sum_{j\geq 1} \gamma_j(t)c_j(x) + \eta_j(t)s_j(x). \tag{9}$$

By introducing the infinite vectors and matrix

$$\boldsymbol{w}(x) = \begin{pmatrix} c_0(x) \\ c_1(x) \\ s_1(x) \\ c_2(x) \\ s_2(x) \\ \vdots \end{pmatrix}, \qquad \boldsymbol{q}(t) = \begin{pmatrix} \gamma_0(t) \\ \gamma_1(t) \\ \eta_1(t) \\ \gamma_2(t) \\ \eta_2(t) \\ \vdots \end{pmatrix}, \qquad D = \frac{2\pi}{b-a} \begin{pmatrix} 0 & & & & \\ & 1\cdot\begin{pmatrix} 1 & \\ & 1 \end{pmatrix} & & & \\ & & 2\cdot\begin{pmatrix} 1 & \\ & 1 \end{pmatrix} & & \\ & & & \ddots & \end{pmatrix}, \tag{10}$$

one obtains that (9) can be rewritten as $u(x,t) = \boldsymbol{w}(x)^\top \boldsymbol{q}(t)$, and the problem can be cast as the infinite-dimensional Hamiltonian ODE problem (where, as is usual, the dot denotes the time derivative)

$$\dot{\boldsymbol{q}}(t) = \boldsymbol{p}(t), \qquad \dot{\boldsymbol{p}}(t) = -D^2\boldsymbol{q}(t) - \int_a^b \boldsymbol{w}(x) f'(\boldsymbol{w}(x)^\top \boldsymbol{q}(t))\mathrm{d}x, \tag{11}$$

with Hamiltonian function

$$H(\boldsymbol{q},\boldsymbol{p}) = \frac{1}{2}\boldsymbol{p}^\top\boldsymbol{p} + \frac{1}{2}\boldsymbol{q}^\top D^2\boldsymbol{q} + \int_a^b f(\boldsymbol{w}(x)^\top\boldsymbol{q})\mathrm{d}x. \tag{12}$$

The following result can be easily proved, by considering that

$$\begin{aligned} v(x,t) &= u_t(x,t) = \boldsymbol{w}(x)^\top\dot{\boldsymbol{q}}(t) \equiv \boldsymbol{w}(x)^\top\boldsymbol{p}(t), \\ u_x(x,t) &= \boldsymbol{w}'(x)^\top\boldsymbol{q}(t) \equiv \left[\tilde{D}\,\boldsymbol{w}(x)\right]^\top\boldsymbol{q}(t), \qquad \tilde{D} = \frac{2\pi}{b-a}\begin{pmatrix} 0 & & & \\ & 1\cdot\begin{pmatrix} & -1 \\ 1 & \end{pmatrix} & & \\ & & 2\cdot\begin{pmatrix} & -1 \\ 1 & \end{pmatrix} & \\ & & & \ddots \end{pmatrix}, \end{aligned} \tag{13}$$

with $\tilde{D}^\top = -\tilde{D}$ and $\tilde{D}D = D\tilde{D}$.

Theorem 2 *The Hamiltonian (12) is equivalent to (5), via the expansion (9). Similarly, the momentum (7) is equivalent to:*

$$I(\boldsymbol{q},\boldsymbol{p}) = \boldsymbol{q}^\top\tilde{D}\boldsymbol{p}. \tag{14}$$

Both (12) and (14) are constant of motion for the solution of (11).

In order for numerically solving problem (11), the series in the expansion (9) is truncated after N terms.[5] In so doing, the vectors and matrices in (10)–(13) become of dimension $2N+1$. The equation to be solved still remains formally (11), the system being now of dimension $4N+2$, by imposing that the residual be orthogonal to the functional subspace

$$\mathcal{V}_N = \mathrm{span}\,\{\,c_0(x),\ c_1(x),\ s_1(x),\ \ldots,\ c_N(x),\ s_N(x)\,\}, \tag{15}$$

which contains the approximation to the solution. Moreover, Theorem 2 still continues to hold true, even though now the truncated invariants are only approximations to the corresponding original ones. Also, in order to obtain a practical computational procedure, the integrals in (11) will be approximated, up to round-off, by using a composite trapezoidal sum defined at the discrete points

$$x_i = a + i(b-a)/m, \qquad i = 0,\ldots,m, \tag{16}$$

which is known to quickly approximate the corresponding integrals, provided that f is suitably regular [4, 6].[6] Consequently, in the sequel we shall assume m to be large enough to assure this requirement. In such a case, by using a classical result [20], any symplectic Runge-Kutta method, applied to solve the truncated version of (11), will conserve the quadratic invariant (14) in the discrete solution while, in general, fails to conserve the invariant (12).

[5] Clearly, the value of N has to meet suitable accuracy requirements for the approximate solution (see, e.g., [4, 14]).

[6] If the integrals are not approximated to machine accuracy, then (12) and (14) are no more conserved.

SPACE SEMI-DISCRETIZATION FOR THE SCHRÖDINGER EQUATION

In the case of the problem (2)-(4), by using the same basis functions (8), one obtains the expansions (9) and

$$v(x,t) = \alpha_0(t)c_0(x) + \sum_{j\geq 1} \alpha_j(t)c_j(x) + \beta_j(t)s_j(x). \tag{17}$$

In such a case, by using the same vectors and matrix defined in (10), as well as the additional infinite vector

$$\boldsymbol{p}(t) = \left(\begin{array}{ccccccc} \alpha_0(t), & \alpha_1(t), & \beta_1(t), & \alpha_2(t), & \beta_2(t), & \ldots \end{array} \right)^\top, \tag{18}$$

one obtains that

$$u(x,t) = \boldsymbol{w}(x)^\top \boldsymbol{q}(t), \qquad v(x,t) = \boldsymbol{w}(x)^\top \boldsymbol{p}(t),$$

and the problem can be rewritten as:

$$\begin{aligned} \dot{\boldsymbol{q}}(t) &= D^2\boldsymbol{p}(t) - \int_a^b \boldsymbol{w}(x) f'\left((\boldsymbol{w}(x)^\top \boldsymbol{q}(t))^2 + (\boldsymbol{w}(x)^\top \boldsymbol{p}(t))^2\right) \boldsymbol{w}(x)^\top \boldsymbol{p}(t)\,\mathrm{d}x, \\ \dot{\boldsymbol{p}}(t) &= -D^2\boldsymbol{q}(t) + \int_a^b \boldsymbol{w}(x) f'\left((\boldsymbol{w}(x)^\top \boldsymbol{q}(t))^2 + (\boldsymbol{w}(x)^\top \boldsymbol{p}(t))^2\right) \boldsymbol{w}(x)^\top \boldsymbol{q}(t)\,\mathrm{d}x, \end{aligned} \tag{19}$$

which is Hamiltonian with Hamiltonian function

$$H(\boldsymbol{q},\boldsymbol{p}) = \frac{1}{2}\left[\boldsymbol{p}^\top D^2 \boldsymbol{p} + \boldsymbol{q}^\top D^2 \boldsymbol{q} - \int_a^b f\left((\boldsymbol{w}(x)^\top \boldsymbol{q})^2 + (\boldsymbol{w}(x)^\top \boldsymbol{p})^2\right)\mathrm{d}x\right]. \tag{20}$$

The following result is analogous to Theorem 2 for the present problem.

Theorem 3 *The Hamiltonian (20) is equivalent to (6), via the expansions (9) and (17). Similarly, the mass functional (7) is equivalent to:*

$$M(\boldsymbol{q},\boldsymbol{p}) = \int_a^b \left((\boldsymbol{w}(x)^\top \boldsymbol{q})^2 + (\boldsymbol{w}(x)^\top \boldsymbol{p})^2\right)\mathrm{d}x. \tag{21}$$

Both (20) and (21) are constant of motion for the solution of (19).

As done in the case of the semilinear wave equation, in order to practically solve problem (19), one has to truncate the series in (9) and (17) to finite sums with N terms. Consequently, the approximate solution will belong to the subspace (15) and, by requiring the residual be orthogonal to it, one obtain again a system of $4N + 2$ differential equations, formally still given by (19), with the vectors and the matrix in (10)-(18) now having dimesion $2N + 1$. Again, to approximate the integrals in (19) we make use of the composite trapezoidal rule defined on the abscissae (16), with m large enough to obtain full machine accuracy, which will be assumed in the sequel.

We end this section by observing that, also in this case, the use of a symplectic Runge-Kutta method for solving (19) guarantees the conservation of the quadratic invariant (21) in the numerical solution but, in general, not that of the Hamiltonian (20).

HAMILTONIAN BOUNDARY VALUE METHODS (HBVMS)

In this section, we briefly sketch the basic facts about the class of energy-conserving Runge-Kutta methods named *Hamiltonian Boundary Value Methods (HBVMs)*, recently devised and studied in [3, 7, 8, 9, 10, 11, 12] for numerically solving Hamiltonian ODE problems. Such methods, which are based on the concept of *discrete line integral* [15, 16, 17], have been also generalized to other conservative problems [1, 2], as well as to cope with the conservation of multiple invariants [5, 11, 13]. As said above, we refer to the monograph [6] for a comprehensive introduction to this subject.

Let us then consider a Hamiltonian ODE problem,

$$\dot{y} = J\nabla H(y) \equiv f(y), \qquad y(0) = y_0 \in \mathbb{R}^{2m}, \qquad J = \left(\begin{array}{cc} & I_m \\ -I_m & \end{array} \right),$$

with $H(y)$ the Hamiltonian function. Since the integrator we are going to describe is a one-step method, it is enough to skecth the first integration step, from $t_0 = 0$ to $t_1 = h$, where h is the timestep. We look for a polynomial approximation σ, having degree s, such that:

$$\sigma(0) = y_0, \qquad \sigma(h) =: y_1 \approx y(h), \qquad H(y_1) = H(y_0).$$

By considering the expansion

$$\dot{\sigma}(ch) = \sum_{j=0}^{s-1} P_j(c)\gamma_j, \qquad c \in [0,1],$$

along the orthonormal Legendre polynomials basis $\{P_j\}_{j\geq 0}$ on $[0,1]$ (i.e., $\int_0^1 P_i(x)P_j(x)\mathrm{d}x = \delta_{ij}$, the Kronecker delta), one obtains:

$$\sigma(ch) = y_0 + h\sum_{j=0}^{s-1}\int_0^c P_j(x)\mathrm{d}x\,\gamma_j, \qquad c \in [0,1], \qquad y_1 \equiv \sigma(h) = y_0 + h\gamma_0,$$

and, by using a corresponding line integral,

$$H(y_1) - H(y_0) \equiv H(\sigma(h)) - H(\sigma(0)) = h\int_0^1 \nabla H(\sigma(ch))^\top \dot{\sigma}(ch)\mathrm{d}c = h\sum_{j=0}^{s-1}\left[\int_0^1 \nabla H(\sigma(ch))P_j(c)\mathrm{d}c\right]^\top \gamma_j.$$

Energy conservation is then gained by setting

$$\gamma_j := J\int_0^1 \nabla H(\sigma(ch))P_j(c)\,\mathrm{d}c \equiv \int_0^1 f(\sigma(ch))P_j(c)\,\mathrm{d}c, \qquad j = 0,\ldots,s-1, \tag{22}$$

due to the fact that $J^\top = -J$. In order to obtain a numerical method from (22), the involved integrals are approximated by using a Gauss-Legendre formula based at the k Gauss-Legendre points $c_1,\ldots,c_k$.[7] In such a case, by setting $Y_i := \sigma(c_i h)$, $i = 1,\ldots,k$, one obtains a k-stage Runge-Kutta method (with stages $\{Y_i\}$), which is named *k-stage Hamiltonian Boundary Value Method of degree s*, in short *HBVM(k,s)*. By setting $\boldsymbol{b} = (b_1,\ldots,b_k)^\top$ and $\boldsymbol{c} = (c_1,\ldots,c_k)^\top$ the vectors with the k Gauss-Legendre weights and abscissae, respectively, it is possible to see that the Butcher tableau of a HBVM(k,s) method is given by

$$\frac{\boldsymbol{c} \;\big|\; \mathcal{I}_s\mathcal{P}_s^\top\Omega}{\;\big|\; \boldsymbol{b}^\top}, \qquad \text{with} \qquad \mathcal{I}_s = \left(\int_0^{c_i} P_{j-1}(x)\mathrm{d}x\right),\ \mathcal{P}_s = \Big(P_{j-1}(c_i)\mathrm{d}x\Big) \in \mathbb{R}^{k\times s}, \quad \Omega = \mathrm{diag}\,(\boldsymbol{b})\,,$$

as well as to prove the following result [10].

Theorem 4 *For all $k \geq s$, a HBVM(k,s) method:*

- *has order $2s$;*
- *when $k = s$ it reduces to the s-stage Gauss collocation method;*
- *is energy-conserving for all polynomial Hamiltonians of degree not larger than $2k/s$. For general and sufficiently regular Hamiltonians, one obtains: $H(y_1) - H(y_0) = O(h^{2k+1})$.*

From the last point one easily realizes that energy conservation can always be obtained for polynomial Hamiltonians while, for general ones, a *practical energy-conservation* be gained by choosing k large enough so that $H(y_1) - H(y_0)$ is within round-off errors. Moreover, this can be done by retaining a computational cost similar to that of the basic s-stage Gauss collocation method ($k = s$), as one easily infers from the fact the the nonlinear system (22) has (block) dimension s, independently of the number k of the Legendre points used for approximating the involved integrals (see [8, 3] for more details).

It is worth mentioning that the implementation of HBVM(k,s) methods for solving both (11) and (19) can be made very efficient, though we shall not consider this issue here (see [4], for the case of the semilinear wave equation).

[7] I.e., $P_k(c_i) = 0,\ i = 1,\ldots,k,$ with P_k the k-th Legendre polynomial.

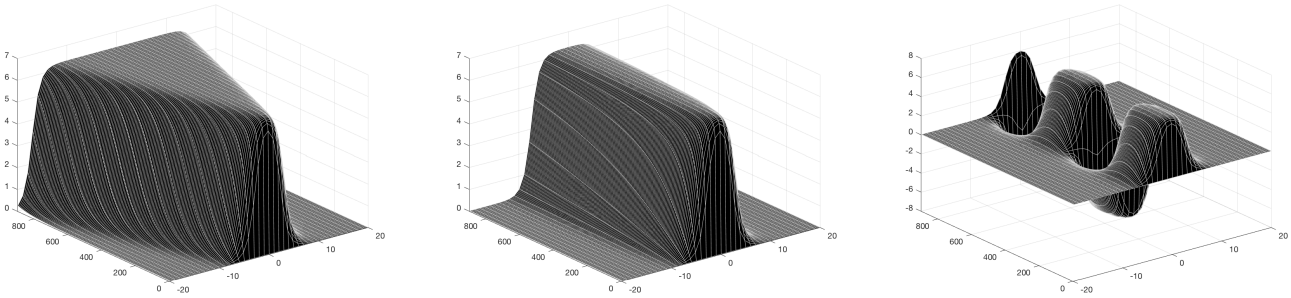

FIGURE 1. Soliton solutions of the sine-Gordon problem: kink-antikink (left); double pole (center); breather (right).

NUMERICAL TESTS

In this section we report a few numerical test, aimed at giving evidence of the fact that energy-conserving methods may be more reliable than other methods (e.g., symplectic ones), for the numerical solution of Hamiltonian PDEs such as (1) and (2). Let us consider, at first, the so called *sine-Gordon equation*, with periodic boundary conditions,

$$u_{tt}(x,t) = u_{xx}(x,t) - \sin(u(x,t)), \qquad (x,t) \in \Omega \equiv [-20,20] \times [0,\infty), \tag{23}$$

possessing soliton solutions, when the initial conditions are prescribed as follows [4]:

$$u(x,0) = 0, \qquad u_t(x,0) = \frac{4}{\gamma}\,\mathrm{sech}\left(\frac{x}{\gamma}\right), \tag{24}$$

with γ a positive parameter. In particular:

- for $0 < \gamma < 1$ one obtains a *kink-antikink* soliton (see the left plot in Fig. 1, for $\gamma = 0.9999$);
- for $\gamma = 1$ one obtains a *double-pole* soliton (see the plot at the center of Fig. 1);
- for $\gamma > 1$ one obtains a *breather* soliton (see the right plot in Fig. 1, for $\gamma = 1.0001$).

Moreover, it turns out that the Hamiltonian (5) is a decreasing function of the parameter γ (see the left plot in Fig. 2). Consequently, energy-conservation could be an issue, when numerically solving problem (23)-(24) with $\gamma = 1$, since nearby values of the Hamiltonian may produce a qualitatively wrong approximation.

We first solve the problem, in the case $\gamma = 1$, by means of the HBVM(2,2) method (i.e., the symplectic 2-stage Gauss collocation method), by using the following parameters:

$$N = 100, \qquad m = 201, \qquad h = 0.3, \qquad nsteps = 3000, \tag{25}$$

where N defines the dimension, $2N+1$, of the approximation space (15), m defines the number of points (16) used for approximating the integrals, h is the timestep, and *nsteps* is the number of integration steps. In so doing, one obtains an energy error of approximately $8 \cdot 10^{-4}$ (its correct value is $H_0 = 16$) and a momentum error of $3 \cdot 10^{-14}$ (its correct value is $I_0 = 0$). However, the numerical energy turns out to be larger than the correct value H_0, so that we obtain a kink-antikink approximation to the solution, as is shown in the plot at the center of Fig. 2. On the contrary, by using the HBVM(8,2) method, with the same parameters as in (25), the method turns out to be practically energy-conserving (the maximum energy error is less than $2 \cdot 10^{-14}$). Moreover, also the momentum error turns out to be very small (less than 10^{-13}), because of the symmetry of the solution, and the computed solution turns out to be correct, as is shown in the plot on the right in Fig. 2.

Let us now consider the nonlinear Schrödinger equation (2), defined with the periodic boundary conditions (4) on the same domain as in (23). In particular, we consider:

$$f(s) = 0.2526896 \cdot s^6, \qquad u_0(x) = \frac{1}{\cosh(x)}, \qquad v_0(x) = 0,$$

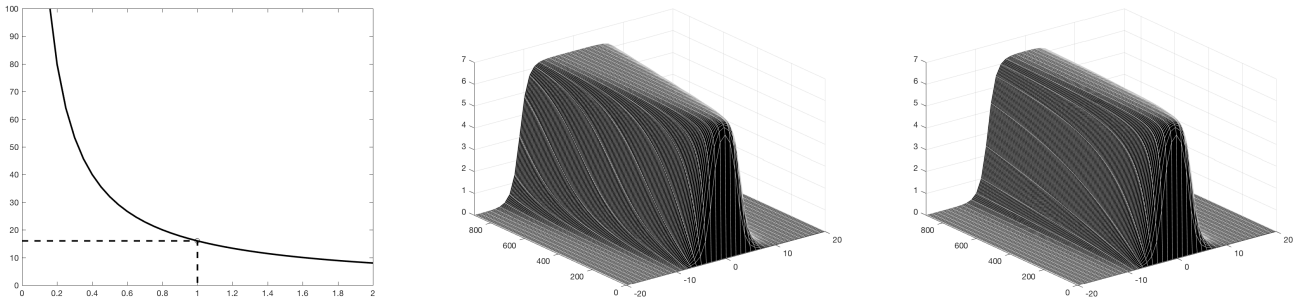

FIGURE 2. Sine-Gordon problem: Hamiltonian versus the parameter γ (left); numerical solution, when $\gamma = 1$, computed by HBVM(2,2) (center); numerical solution, when $\gamma = 1$, computed by HBVM(8,2) (right).

which produce a solution with a blow-up around $t^* \approx 2$, as it can be seen in the left plot of Fig. 3. The corresponding Hamiltonian value is $H_0 \approx 0.24$, whereas the mass has a value $M_0 = 2$. If we use the HBVM(10,2) method, with parameters (their meaning being the same as in (25))

$$N = 100, \qquad m = 1001, \qquad h = 0.1, \qquad nsteps = 1000, \tag{26}$$

then the numerical solution (correctly) blows-up after 20 integration steps, with an energy error of $2 \cdot 10^{-16}$ and a mass error $2 \cdot 10^{-4}$. On the other hand, by using the (symplectic) HBVM(2,2) method with the same parameters as in (26), one obtains an energy error $2 \cdot 10^{-6}$ and a mass error $7 \cdot 10^{-15}$ but, in this case, the numerical solution *doesn't* blow-up, as is shown in the plot on the right of Fig. 3. In fact, one may see that all the 1000 integration steps are performed by the method. Consequently, even though the mass is conserved,[8] nevertheless, the Hamiltonian error is responsible for the wrong qualitative behavior of the numerical approximation.

CONCLUSIONS

From the numerical tests reported above, one concludes that energy-conserving methods may be more reliable than other (e.g., symplectic) integrators, when solving Hamiltonian PDEs. Moreover, also the possibility of preserving multiple conservation laws could be of interest (see, e.g., [19, 25]). In this respect, multiple invariants-conserving line integral methods, such as those defined in [5, 13] , could be considered. However, in the case of the equations studied here, where the additional invariants are quadratic, the methods described in [11] could be the best choice. For this reason, their application to Hamiltonan PDEs, as well as their efficient implementation, will be the subject of future investigations.

REFERENCES

[1] P. Amodio, L. Brugnano, F. Iavernaro. *Adv. Comput. Math.* **41** (2015) 881–905.
[2] L. Brugnano, M. Calvo, J.I. Montijano, L. Ràndez. *J. Comput. Appl. Math.* **236** (2012) 3890–3904.
[3] L. Brugnano, G. Frasca Caccia, F. Iavernaro. *Numer. Algor.* **65** (2014) 633–650.
[4] L. Brugnano, G. Frasca Caccia, F. Iavernaro. *Appl. Math. Comput.* **270** (2015) 842–870.
[5] L. Brugnano, F. Iavernaro. *J. Comput. Appl. Math.* **236** (2012) 3905–3919.
[6] L. Brugnano, F. Iavernaro. *Line Integral Methods for Conservative Problems*. Chapman and Hall/CRC, Boca Raton, FL, 2016.
[7] L. Brugnano, F. Iavernaro, D. Trigiante. *J. Numer. Anal. Ind. Appl. Math.* **5**, 1-2 (2010) 17–37.
[8] L. Brugnano, F. Iavernaro, D. Trigiante. *J. Comput. Appl. Math.* **236** (2011) 375–383.
[9] L. Brugnano, F. Iavernaro, D. Trigiante. *Appl. Math. Comput.* **218** (2012) 8053–8063.
[10] L. Brugnano, F. Iavernaro, D. Trigiante. *Appl. Math. Comput.* **218** (2012) 8475–8485.

[8] I.e., in the right-plot of Fig. 3, the integral over x, from -20 to 20, is always equal to 2, at each integration step.

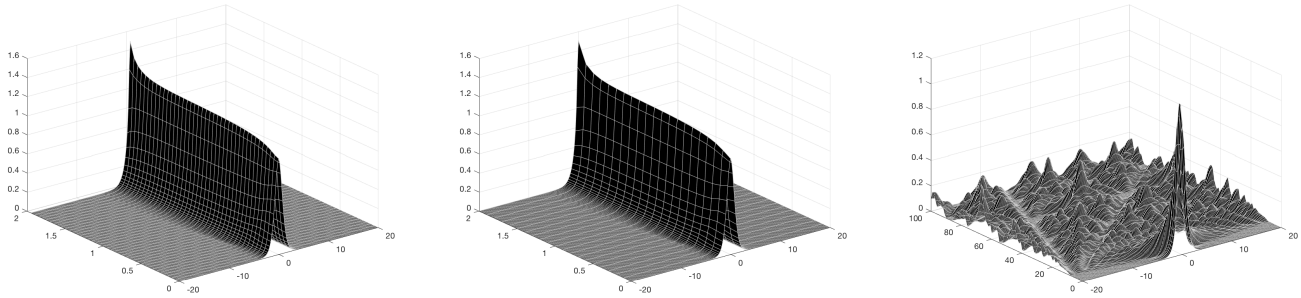

FIGURE 3. Schödinger equation, plot of $u(x,t)^2 + v(x,t)^2 \equiv |\psi(x,t)|^2$: reference solution (left); numerical solution computed by HBVM(10,2) (center); numerical solution computed by HBVM(2,2) (right).

[11] L. Brugnano, F. Iavernaro, D. Trigiante. *SIAM J. Numer. Anal.* **50**, No. 6 (2012) 2897–2916.

[12] L. Brugnano, F. Iavernaro, D. Trigiante. *Commun. Nonlin. Sci. Numer. Simul.* **20** (2015) 650–667.

[13] L. Brugnano, Y. Sun. *Numer. Algor.* **65** (2014) 611–632.

[14] C. Canuto, M.Y. Hussaini, A. Quarteroni, T.A. Zang. *Spectral Methods in Fluid Dynamics*. Springer-Verlag, New York, 1988.

[15] F. Iavernaro, B. Pace. *s*-stage . *AIP Conf. Proc.* **936** (2007) 603–606.

[16] F. Iavernaro, B. Pace. *AIP Conf. Proc.* **1048** (2008) 888–891.

[17] F. Iavernaro, D. Trigiante. *J. Numer. Anal. Ind. Appl. Math.* **4**,1-2 (2009) 87–101.

[18] B. Leimkulher, S. Reich. *Simulating Hamiltonian Dynamics*. Cambridge University Press, Cambridge, 2004.

[19] H. Li, Y. Wang, Q. Sheng. *Numerical Methods for Partial Differential Equations* (2016) DOI: 10.1002/num.22062

[20] J.M. Sanz-Serna. *BIT* **28** (1988) 877–883.

[21] J.M. Sanz-Serna, M.P. Calvo. *Numerical Hamiltonian Problems*. Chapman & Hall, London, 1994.

[22] Ya.D. Sergeyev. *Arithmetic of Infinity*. Edizioni Orizzonti Meridionali, 2003.

[23] Ya.D. Sergeyev. *Optimization Letters* **5** (2011) 575–585.

[24] Ya.D. Sergeyev. *Appl. Math. Comput.* **219** (2013) 10668–10681.

[25] J. Yan, Z. Zhang. *Comput. Phys. Commun.* **201** (2016) 33–42.